WaveComBE

mmWave Communications in the Built Environments

WaveComBE_D3.1

Report on the fundamental performance limits of dense 3D millimetre-wave small cell deployment

Version v1.0 Date: 23/09/2019

Document properties:

Grant Number:	766231
Document Number:	D3.1
Document Title:	Report on the fundamental performance limits of dense 3D millimeter wave small cell deployment
Partners involved:	University of Sheffield
Authors:	Chen Chen, Yixin Zhang, Xiaoli Chu, Jie Zhang
Contractual Date of Delivery:	2019/09/30
Dissemination level:	PU[1]
Version:	1.0
File Name:	WaveComBE D3.1_v1.0

[1] CO = Confidential, only members of the consortium (including the Commission Services)

PU = Public

Table of contents

Executive Summary

Millimeter wave (mm-Wave) communication is a key candidate technology for 5G cellular mobile networks [1]. This is mainly due to the availability of large spectrum resources in the unlicensed mm-Wave bands, which has the potential to enable much higher data rates than the licensed cellular frequency bands [7-8]. However, communication in mm-Wave bands is facing several challenges such as the increase in path loss with increasing frequency and severe penetration losses through solid materials. To tackle these challenges, large antenna arrays are used to enable beamforming at the transmitter and receiver, which compensates the path loss [2]. To understand the fundamental performance limits of densely deployed indoor mm-Wave small cell networks (SCN), we propose a grid model for indoor massive multiple-input-multiple-output (MIMO) mm-Wave multi-cell networks. Based on the grid model, we maximize the average downlink user (UE) rate and the network energy efficiency (EE) by jointly optimizing the massive MIMO configuration parameters and the base station (BS) density and derive the analytical upper-bounds of the average UE rate and energy efficiency.

The report mainly consists of the following two parts:

Firstly, we derive the analytical expressions of the average downlink UE rate and the EE per cell in an indoor 28 GHz mm-Wave massive MIMO multi-cell scenario, where we consider both line-of-sight (LOS) and non-line-of-sight (NLOS) channels [11-13] that may simultaneously occur in dense mm-Wave SCNs. Different from existing works that usually assume a fixed coverage area for all small cells, our analytical derivation considers the effect of network densification that may change in terms of coverage area per cell.

Secondly, we propose a global optimization algorithm based on a genetic algorithm [6] to achieve a desired trade-off between the sum data rate of all downlink users and the system total power consumption by jointly optimizing the number of antennas per BS, the number of users per cell, the transmission power per antenna, and the BS density, subject to the quality of service (QoS) constraints. We present numerical results to show that as compared with lower frequencies, an indoor mm-Wave massive MIMO SCN can achieve a higher average downlink user rate and a larger EE with less antennas deployed per BS and a smaller coverage area per cell. The accuracy of our derived analytical expressions of the average downlink user rate and the EE per cell is verified through comparison with simulation results.

List of Figures

List of Tables

List of Acronyms and Abbreviations

mm-Wave	millimeter-wave
MIMO	multiple-input multiple-output
BS	base station
EE	energy efficiency
SCN	small cell network
GA	genetic algorithm
LOS	line-of-sight
NLOS	non- line-of-sight
QoS	quality of service
TDD	time-division duplex
ZF	zero-forcing
UE	user equipment
CSI	channel state information

1. System Model

In this section, we introduce the indoor mm-Wave massive MIMO multi-cell network model and the associated channel model.

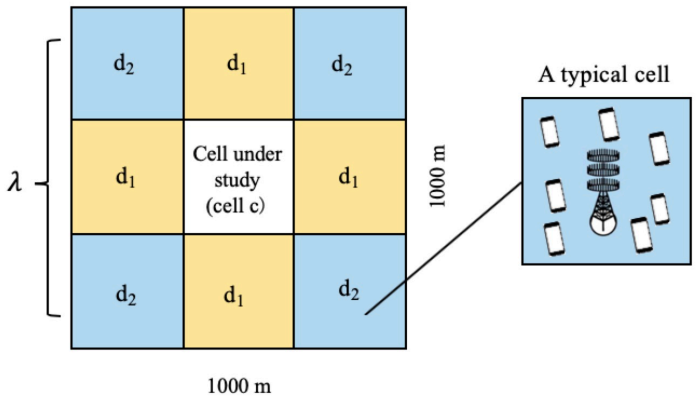

Fig. 1. Illustration of a multi-cell network in a 1000 m x 1000 m square area, wherein the total number of cells is given by λ^2.

1.1 Network model

As shown in Fig. 1, we consider the downlink of an indoor mm-Wave multi-cell massive MIMO network in a 1000m×1000m square area consisting of $C = \lambda^2$ square small cells, where each column of the square grid contains λ cells. The set of these small cells is denoted by $\mathcal{C} = \{1,2,3,\ldots,C\}$. The density of the BSs is given by λ^2 cells/km^2. Each BS uses a co-located array with M antennas to communicate with K single-antenna user equipment (UE) that are served in a round-robin fashion within its coverage area. The transmission power for each antenna is denoted by p. We consider block flat-fading channels where B_C (in Hz) is the coherence bandwidth and T_C (in seconds) is the coherence time. Hence, the channels are static within each time-frequency coherence block of $U = B_C T_C$ symbols. We assume that the BSs and UEs are perfectly synchronized and operate in the time-division duplex (TDD) mode.

1.2 Channel model

The large-scale fading between a UE and a BS is assumed to be the same for all the BS antennas. This assumption is reasonable because the distances between UEs and the BS are much larger than the distance between the antennas. Moreover, we assume that the large-scale fading is dominated by path loss, which is often modeled as

$$l(x) = \frac{\beta_0}{x^\alpha}, \quad (1)$$

where α is the path-loss distance exponent and the constant β_0 regulates the channel attenuation at the unit distance.

An important feature of an mm-Wave channel is the sensitivity to blockages. In outdoor environments, buildings make the path loss much higher for NLOS channels than LOS channels. Letting the LOS probability of a link be $P(R) = e^{-\gamma R}$, where R is the distance from the BS to UE, then the NLOS probability of the link is given by $\big(1 - P(R)\big)$ [5]. Hence, the large-scale fading in the channel model is given by

$$L(R) = \mathbb{I}(P(R))\beta_0^{\mathrm{L}} R^{-\alpha_{\mathrm{L}}} + \mathbb{I}(1 - P(R))\beta_0^{\mathrm{N}} R^{-\alpha_{\mathrm{N}}}, \quad (2)$$

where $\mathbb{I}(x)$ is the Bernoulli random variable with parameter x, β_0^{L} and β_0^{N} are the signal attenuation at reference distance for LOS and NLOS links, respectively, and α_{L} and α_{N} are the path-loss exponents for LOS and NLOS links, respectively.

The M antennas at the BS are adequately spaced from one another such that the channel components between the BS antennas and the single-antenna UEs are uncorrelated. The channel model between the BS and UE k is denoted by the vector $\mathbf{h}_k = [h_{k,1}, h_{k,2}, \ldots, h_{k,M}]^T \in \mathbb{C}^{M\times 1}$, where $h_{k,j}$ is the instantaneous channel coefficient from the jth BS antenna to the kth UE. Rayleigh small-scale fading is assumed and is denoted by $\mathbf{h}_k \sim \mathcal{CN}(\mathbf{0}_M, L(R_k)\mathbf{I}_M)$, where R_k is the distance from the serving BS to UE k, $\mathbf{0}_M$ is an $M \times 1$ zero vector, and $\mathbf{I}_M$ is an $M \times 1$ identity vector. For analytic tractability, we assume that the BS is able to acquire perfect downlink channel state information (CSI) from the uplink pilots.

2. Performance Analysis

In this section, we define and derive the performance metrics including the average downlink user rate and the EE per cell.

2.1 Average downlink user rate

The received signal of UE k in cell c is given by

$$y_{ck} = \mathbf{h}_{cck}^H \sum_{i=1}^{K} \mathbf{w}_{ci}\, s_{ci} + \sum_{d\neq c} \mathbf{h}_{dck}^H \sum_{i=1}^{K} \mathbf{w}_{di}\, s_{di} + \mathbf{n}_{ck}, \tag{3}$$

where $\mathbf{h}_{cck}^H$ is the channel coefficient vector between BS c and UE k in cell c, $\mathbf{w}_{ci}$ is the zero-forcing (ZF) vector from BS c to UE i in cell c, s_{ci} is the transmitted signal from BS c to UE i in cell c, $\mathbf{h}_{dck}^H$ is the channel coefficient vector between BS d and UE k in cell c, $\mathbf{w}_{di}$ is the ZF vector from BS d to UE i in cell c, s_{di} is the transmit signal from BS d to UE i in cell c, and $\mathbf{n}_{ck}$ is the noise vector.

The average downlink data rate achieved by UE k in cell c is given by [4],

$$R_c(M,K,p,\lambda) = B\left(1-\frac{\tau K}{U}\right)\log_2\left(1+\frac{p\frac{M}{K}(M-K)}{\sigma^2 G_{cc}+\sum_{d\neq c} pMG_{cd}}\right), \tag{4}$$

where $\left(1-\frac{\tau K}{U}\right)$ accounts for the necessary overhead for channel estimation, for simplicity we assume the same U for LOS and NLOS, G_{cd} is the average inter-cell interference power from BS d to UE k in cell c, and G_{cc} is the channel variance from the serving BS, which is calculated as

$$\begin{aligned} G_{cc} \;=\; & \int_{x=-r}^{r}\int_{y=-r}^{r} \frac{(x^2+y^2)^{\alpha_{\mathrm{L}}/2} e^{-\gamma\sqrt{x^2+y^2}}}{4r^2\beta_0^{\mathrm{L}}}\,dxdy + \\ & \int_{x=-r}^{r}\int_{y=-r}^{r} \frac{(x^2+y^2)^{\alpha_{\mathrm{N}}/2}\left(1-e^{-\gamma\sqrt{x^2+y^2}}\right)}{4r^2\beta_0^{\mathrm{N}}}\,dxdy \end{aligned} \tag{5}$$

If $\lambda = 1$, then $G_{cd} = 0$. If $\lambda \geq 3$, we define two odd numbers i and j, where $i = 1, 3, \ldots, \lambda-2$, and $j = -1, 1, \ldots, \lambda-2$, and define two functions $f(x,y) = x^2 + y^2$, and $g(x,y) = (x-i-1)^2 + (y-j-1)^2$, then G_{cd} can be computed as follows:

$$\begin{aligned} G_{cd} = & \sum_{i=1}^{\lambda-2}\sum_{j=-1}^{\lambda-2}\int_{x=i}^{i+2}\int_{y=j}^{j+2} \frac{(g(x,y))^{\alpha_{\mathrm{L}}/2} e^{-\gamma\sqrt{f(x,y)}} e^{-\gamma\sqrt{g(x,y)}}}{(f(x,y))^{\alpha_{\mathrm{L}}/2}}\,dxdy + \\ & \sum_{i=1}^{\lambda-2}\sum_{j=-1}^{\lambda-2}\int_{x=i}^{i+2}\int_{y=j}^{j+2} \frac{(g(x,y))^{\alpha_{\mathrm{N}}/2} e^{-\gamma\sqrt{f(x,y)}}\left(1-e^{-\gamma\sqrt{g(x,y)}}\right)}{(f(x,y))^{\alpha_{\mathrm{L}}/2}}\,dxdy + \\ & \sum_{i=1}^{\lambda-2}\sum_{j=-1}^{\lambda-2}\int_{x=i}^{i+2}\int_{y=j}^{j+2} \frac{(g(x,y))^{\alpha_{\mathrm{L}}/2} e^{-\gamma\sqrt{g(x,y)}}\left(1-e^{-\gamma\sqrt{f(x,y)}}\right)}{(f(x,y))^{\alpha_{\mathrm{N}}/2}}\,dxdy + \\ & \sum_{i=1}^{\lambda-2}\sum_{j=-1}^{\lambda-2}\int_{x=i}^{i+2}\int_{y=j}^{j+2} \frac{(g(x,y))^{\alpha_{\mathrm{N}}/2}\left(1-e^{-\gamma\sqrt{f(x,y)}}\right)\left(1-e^{-\gamma\sqrt{g(x,y)}}\right)}{(f(x,y))^{\alpha_{\mathrm{N}}/2}}\,dxdy, \end{aligned} \tag{6}$$

2.2 Energy efficiency

The EE per cell is defined as the number of bits successfully transferred per Joule of energy consumed and hence can be computed as the ratio of the average downlink sum rate (in bit/second) and the average total power consumption (in Joule/s), i.e.,

$$EE(M,K,p,\lambda) = \frac{KR_c(M,K,p,\lambda)}{P_c(M,K,p)}, \quad (7)$$

where $R_c(M,K,p,\lambda)$ is given in (4), $P_c(M,K,p)$ is the total power consumed by a BS, and

$$P_c(M,K,p) = P_{\mathrm{PA},c} + P_{\mathrm{CP},c}, \quad (8)$$

$P_{\mathrm{PA},c}$ is the power amplifier power consumption and $P_{\mathrm{CP},c}$ is the circuit power consumption of BS c, which is given by

$$P_{\mathrm{CP},c} = P_{\mathrm{FIX}} + P_{\mathrm{TC}} + P_{\mathrm{CE}} + P_{\mathrm{ZF}} + P_{\mathrm{C/D}} + P_{\mathrm{BH}}, \quad (9)$$

where the power consumed in the transceiver is given by $P_{\mathrm{TC}} = P_{\mathrm{BS}} + P_{\mathrm{SYN}}$, P_{BS} is the power required to run the circuit components, e.g., converters, mixers and filters attached to each antenna at the BS, P_{SYN} is the power consumed by the local oscillator, P_{CE} is the power required for channel estimation process, $P_{\mathrm{C/D}}$ is the total power required for channel coding and channel decoding, P_{FIX} is the fixed power consumption, P_{BH} is the power consumption for backhaul, and P_{ZF} is the power consumption for beamforming.

Following [3], we rewrite (9) as follows

$$P_{\mathrm{CP},c} = \mathcal{A}KR_c + \sum_{i=0}^{3} \mathcal{C}_i K^i + M \sum_{i=0}^{2} \mathcal{D}_i K^i, \quad (10)$$

where $\mathcal{A} = P_{\mathrm{COD}} + P_{\mathrm{DEC}} + P_{\mathrm{BT}}$, $\mathcal{C}_0 = P_{\mathrm{FIX}} + P_{\mathrm{SYN}}$, $\mathcal{C}_1 = 0$, $\mathcal{C}_2 = 0$, $\mathcal{C}_3 = \frac{B}{3UL_{\mathrm{BS}}}$, $\mathcal{D}_0 = P_{\mathrm{BS}}$, $\mathcal{D}_1 = \frac{B}{L_{\mathrm{BS}}}(2 + \frac{1}{U})$, $\mathcal{D}_2 = \frac{3B}{UL_{\mathrm{BS}}}$.

3. Joint Optimization

In this section, we maximize the EE per cell by jointly optimizing the parameters M, K, p and λ as follows.

$$\max_{M,K,p,\lambda} EE(M,K,p,\lambda), \tag{11}$$

Subject to:

$$C1: M \in \mathbb{Z}_+, K \in \mathbb{Z}_+, \lambda \in \mathbb{Z}_+$$
$$C2: 1 \leq K \leq K_{max}$$
$$C3: K < M \leq M_{max}$$
$$C4: 0 \leq p \leq p_{max}$$
$$C5: 1 \leq \lambda \leq \lambda_{max}$$
$$C6: R_c \geq R_{min}$$

To solve the optimization problem in (11), we propose a GA [6] based scheme as follows.

Initialization: Input K_{max} , M_{max}, p_{max} ,λ_{max} and R_{min}. The initial population is randomly selected from all the possible solutions, where each individual represents a potential optimal solution subject to the constraints in (11). The size of the population is set as 100. Check constraints in (11) for each individual, if the individual fails to satisfy the constraints, then repeat the mutation step until it satisfies the constraints.

Selection: In this stage, chromosomes in current population are selected for later crossover. The most common employed method for selection is roulette, where the probability of choosing a chromosome is proportional to its fitness.

Crossover: To avoid falling into local optimization, it is necessary to diverge the selected population. Similar to the biological reproduction in evolution, the individuals exchange their information to generate new population. The chromosomes will be selected according to the crossover probability ρ_c. During crossover, a random point is randomly selected, then the parent chromosomes will exchange their data at the chosen point. The new chromosomes after exchange are called offspring chromosomes. Check constraints in (11) for each individual, if the individual fails to satisfy the constraints, then repeat the mutation step until it satisfies the constraints.

Mutation: Similar with crossover, mutation is designed to ensure the diversity of the population. For each value in the chromosome, a probability of mutation ρ_m is applied to decide whether this value should undergo mutation or not. The mutation step is important to avoid the premature convergence of the whole algorithm. Check constraints in (11) for each individual, if the individual fails to satisfy the constraints, then repeat the mutation step until it satisfies the constraints.

Termination: The algorithm will terminate when the pre-defined maximum number of iterations is reached or an optimal result has been achieved.

4. Simulation Results

The parameters for our simulation are given in Tables 1-3 [3], [5].

Table 1. Parameters for a mm-Wave small cell network

Parameter	Value
Transmission bandwidth: B	100 MHz
Channel coherence bandwidth: B_{C}	10 MHz
Channel coherence time: T_{C}	0.7 ms
Total noise power: $B\sigma^2$	-89 dBm
LOS path loss at reference distance: β_0^{L}	$10^{-6.14}$
NLOS path loss at reference distance: β_0^{N}	$10^{-7.11}$
LOS path loss exponent: α_{L}	2.5
NLOS path loss exponent: α_{N}	5

Table 2. Parameters for a microwave frequency network

Parameter	Value
Transmission bandwidth: B	20 MHz
Channel coherence bandwidth: B_{C}	180 kHz
Channel coherence time: T_{C}	10 ms
Total noise power: $B\sigma^2$	-96 dBm
Path loss at reference distance: β	$10^{-3.85}$
Path loss exponent:α	3

Table 3. Parameters for the power consumption model

Parameter	Value
Computational efficiency at BS: L_{BS}	12.8 Gflops/W
PA efficiency at BS: η	0.39
Fixed power consumption: P_{FIX}	18 W
Power consumption by local oscillator: P_{SYN}	2 W
Power required for circuit components at BS: P_{BS}	1 W
Power required for coding: P_{COD}	0.1 W/(Gbit/s)
Power required for decoding: P_{DEC}	0.8 W/(Gbit/s)
Power required for backhaul: P_{BT}	0.25 W/(Gbit/s)

In the simulation, we consider an indoor 28 GHz mm-Wave massive MIMO SCN with a bandwidth of 100 MHz. The pilot length for our model is 1. We assume an initial combination of M, K, λ and p to be 100, 10, 21 and 0.07 W respectively. Then we increase the value of M from 11 to 200 to obtain Fig. 2(a). It is observed that the EE per cell is a quasi-concave function of M while the average user rate increases monotonically. From Fig. 2(b) and Fig. 2(c), we can see that the EE per cell is a quasi-concave function. The average downlink user rate monotonically decreases with K and increases with p. In Fig. 2(d), the EE per cell and the average downlink user rate both decrease slightly after they have reached the maximum value, so they are both quasi-concave functions. It is observed that the maximum downlink user rate may exceed 500 Mbit/s. From Fig. 2(a), we can see that the downlink user rate can always increase with increasing number of antennas.

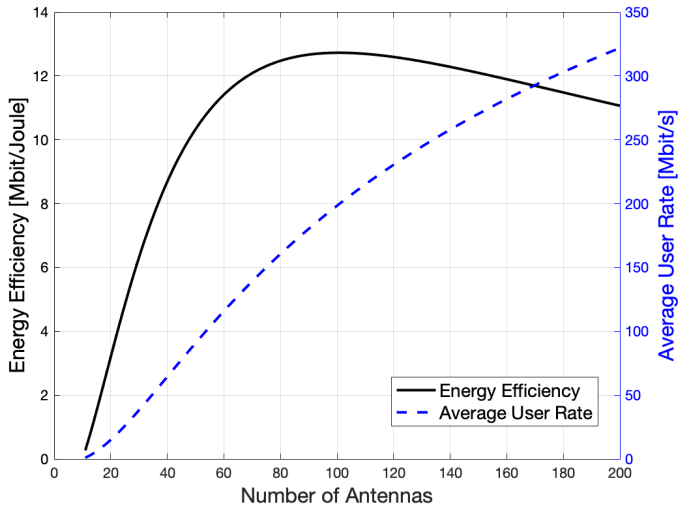

(a)

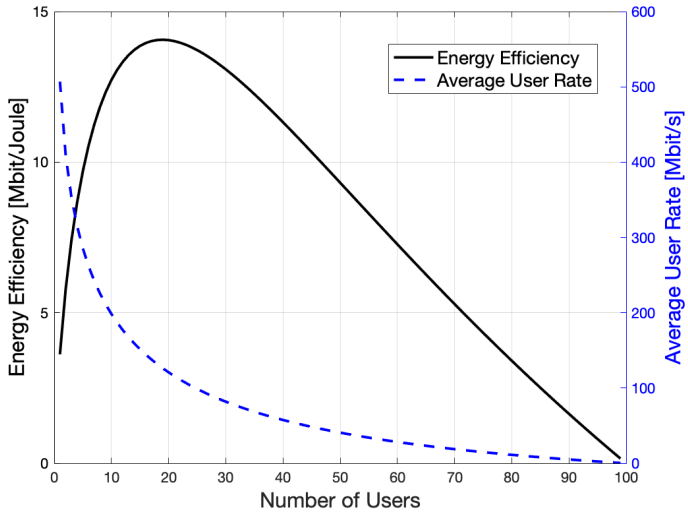

(b)

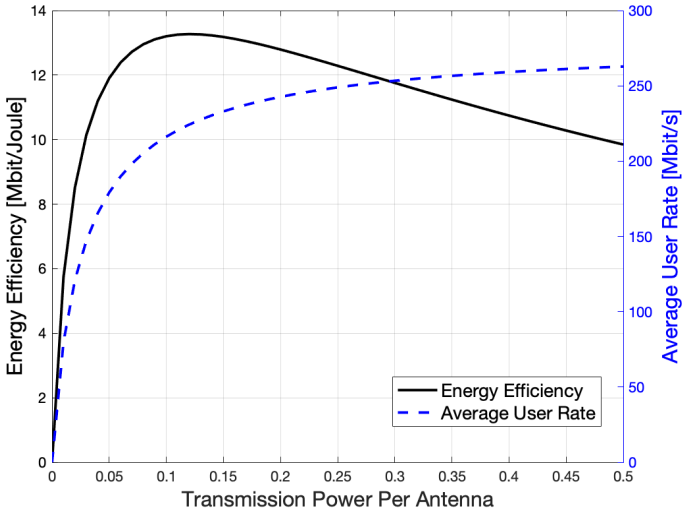

(c)

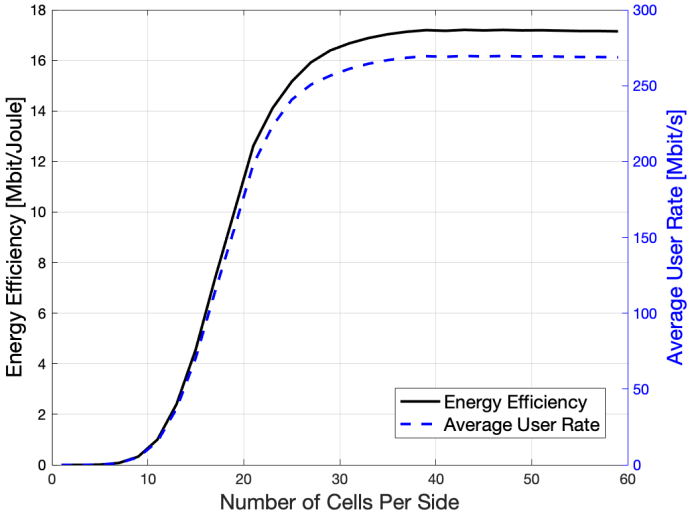

(d)

Fig. 2. Impact of different system parameters on the EE per cell and average downlink user rate.

Next, we compare our proposed scheme with the scheme in reference [3] and a microwave frequency SCN (i.e., with a carrier frequency of 2 GHz). For the constraints in (11), we assume $K_{max} = 100$, $M_{max} = 250$, $p_{max} = 0.5$ W, the user rate threshold $R_{min} = 100$ Mbit/s, and the maximum power for the BS $P_{max} = 10$ W. As shown in Fig. 3, our proposed scheme can achieve a much higher EE than the reference scheme in [3]. This illustrates the importance of optimizing the density of BSs [9-10]. In addition, our scheme achieves more than twice the EE of the microwave frequency SCN, showing the advantage of using mm-Wave communication. The simulation results validate that combining mm-Wave, massive MIMO, and dense SCN can bring gains in energy efficiency. The upper bound of the EE per cell is 17.584 Mbit/Joule.

In Fig. 4, we show that an indoor mm-Wave massive MIMO SCN can provide a much higher downlink user rate than an indoor microwave MIMO SCN. However, the improvement of EE may sacrifice downlink user rate. This implies that we need to study more advanced power saving technique to meet the high-data-rate requirements of 5G.

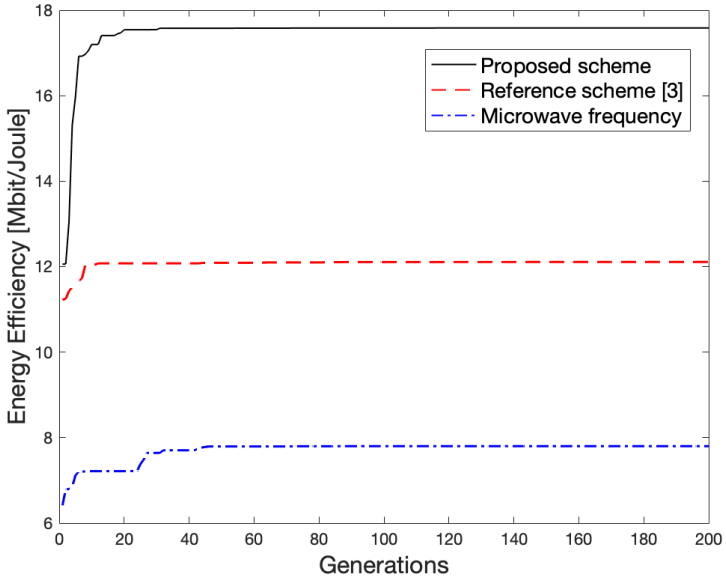

Fig. 3. Comparison of energy efficiency per cell achieved by different schemes

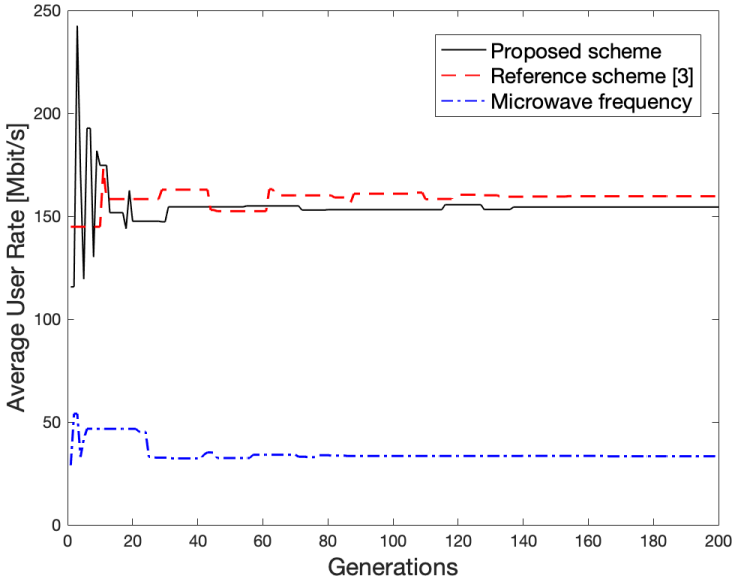

Fig. 4. Comparison of average downlink user rate while achieving the maximal EE

5. Conclusions

In this report, we have analysed the performance of indoor mm-Wave massive MIMO dense SCNs and have derived the expressions for the average downlink user rate and the EE per cell. We have proposed a GA based scheme to obtain the maximum EE per cell by jointly optimizing the number of antennas per BS, the number of users per cell, the transmission power per antenna, and the density of BSs in the indoor mm-Wave massive MIMO SCN. The numerical and simulation results show that our proposed scheme can achieve a much higher EE per cell and a higher average downlink user rate than the existing scheme [3] and a microwave frequency SCN, which validates the advantage of deploying dense mm-Wave massive MIMO SCNs in indoor environments. Our analytical and simulation results show that the average downlink UE rate gain can always be obtained through increasing the number of antennas per BS, and the upper bound for the EE per cell is 17.584 Mbit/Joule. In our future work, we will extend the proposed analytical framework to 3D indoor scenarios and to optimise the massive MIMO configurations for indoor mm-Wave small cell deployment.

References

[1] J. G. Andrews et al., "What will 5G be?" *IEEE J. Sel. Areas Commun.*, vol. 32, no. 6, pp. 1065-1082, Jun. 2014.

[2] E. Björnson, L. Sanguinetti and M. Kountouris, "Deploying dense networks for maximal energy efficiency: small cells meet massive MIMO,'' *IEEE J. Sel. Areas Commun.*, vol. 34, no. 4, pp. 832-847, Apr. 2016.

[3] E. Björnson, L. Sanguinetti, J. Hoydis and M. Debbah, "Optimal design of energy-efficient multi-user MIMO systems: is massive MIMO the answer?'' *IEEE Trans. Wireless Commun.*, vol. 14, no. 6, pp. 3059-3075, Jun. 2015.

[4] M. M. A. Hossain, C. Cavdar, E. Björnson and R. Jäntti, "Energy saving game for massive MIMO: coping with daily load variation,'' *IEEE Trans. Veh.Technol.*, vol. 67, no. 3, pp. 2301-2313, Mar. 2018.

[5] T. Bai and R. W. Heath, "Coverage and rate analysis for millimeter-wave cellular networks," *IEEE Trans. Wireless Commun.,* vol. 14, no. 2, pp. 1100-1114, Feb. 2015.

[6] N. Sharma and A. S. Madhukumar, "Genetic algorithm based proportional fair resource allocation in multicast OFDM systems," *IEEE Trans. Broadcast*., vol. 61, no. 1, pp. 16-29, Mar. 2015.

[7] C. Li, J. Zhang and K. B. Letaief, "Throughput and energy efficiency analysis of small cell networks with multi-antenna base stations," *IEEE Trans. Wireless Commun.*, vol. 13, no. 5, pp. 2505-2517, May. 2014.

[8] Y. Yan, H. Gao, T. Lv and Y. Lu, "Energy-efficient resource allocation in ultra-dense networks with massive MIMO," *IEEE Globecom Workshops (GC WS),* Singapore, 2017, pp. 1-7.

[9] J. Zhang and G. d. l. Roche, "Femtocells: technologies and deployment," *John Wiley and Sons,* 2010.

[10] T. Nakamura *et al.*, "Trends in small cell enhancements in LTE advanced," *IEEE Commun. Mag.*, vol. 51, no. 2, pp. 98-105, Feb. 2013.

[11] T. Bai, R. Vaze, and R. W. Heath, "Analysis of blockage effects on urban cellular networks,'" *IEEE Trans. Wireless Commun.,* vol. 13, no. 9, pp. 5070-5083, Sep. 2014.

[12] A. Thornburg, T. Bai and R. W. Heath, "Performance analysis of outdoor mmWave ad hoc networks," *IEEE Trans. Signal Process.,* vol. 64, no. 15, pp. 4065-4079, Aug. 2016.

[13] J. Liu, M. Sheng and J. Li, "Improving network capacity scaling law in ultra-dense small cell networks," *IEEE Trans. Wireless Commun*., vol. 17, no. 9, pp. 6218-6230, Sept. 2018.